Metrol. Meas. Syst., Vol. 29 (2022) No. 1, pp. 175–190
DOI: 10.24425/mms.2022.138551

PAN POLSKA AKADEMIA NAUK

METROLOGY AND MEASUREMENT SYSTEMS

Index 330930, ISSN 0860-8229
www.metrology.wat.edu.pl

M&MS

AUTOMATIC IDENTIFICATION OF MALFUNCTIONS OF LARGE TURBOMACHINERY DURING TRANSIENT STATES WITH GENETIC ALGORITHM OPTIMIZATION

Tomasz Barszcz[1)], Mateusz Zabaryłło[2)]

1) *AGH University of Science and Technology, Al. Mickiewicza 30, 30-059 Kraków, Poland,* (*tbarszcz@agh.edu.pl*)
2) *GE Power, ul. Stoczniowa 2, 82-300 Elbląg, Poland,* (✉ *mateusz.zabaryllo1@ge.com* +48 783 578 453)

Abstract

Turbines and generators operating in the power generation industry are a major source of electrical energy worldwide. These are critical machines and their malfunctions should be detected in advance in order to avoid catastrophic failures and unplanned shutdowns. A maintenance strategy which enables to detect malfunctions at early stages of their existence plays a crucial role in facilities using such types of machinery. The best source of data applied for assessment of the technical condition are the transient data measured during start-ups and coast-downs. Most of the proposed methods using signal decomposition are applied to small machines with a rolling element bearing in steady-state operation with a shaft considered as a rigid body. The machines examined in the authors' research operate above their first critical rotational speed interval and thus their shafts are considered to be flexible and are equipped with a hydrodynamic sliding bearing. Such an arrangement introduces significant complexity to the analysis of the machine behavior, and consequently, analyzing such data requires a highly skilled human expert. The main novelty proposed in the paper is the decomposition of transient vibration data into components responsible for particular failure modes. The method is automated and can be used for identification of turbogenerator malfunctions. Each parameter of a particular decomposed function has its physical representation and can help the maintenance staff to operate the machine properly. The parameters can also be used by the managing personnel to plan overhauls more precisely. The method has been validated on real-life data originating from a 200 MW class turbine. The real-life field data, along with the data generated by means of the commercial software utilized in GE's engineering department for this particular class of machines, was used as the reference data set for an unbalanced response during the transients in question.

Keywords: machine learning, fault detection, transient, turbine generator, genetic algorithm.

1. Introduction

Large sets of turbogenerators are the main contributors in respect of the worldwide electric generation. Although renewable energy sources have been rapidly expanding in recent years, huge power plants with large turbogenerators still play an overwhelming role in the power

Article history: received August 26, 2021; revised October 28, 2021; accepted December 10, 2021; available online December 19, 2021.

generation industry. Such a scenario, according to specific forecasts, is likely to be maintained for at least a few decades. The truth is that turbines coupled with generators appear to be the main machines in every single power plant all over the world. Their ability to produce is critical for the entire power generation process. Such important units are called "critical machines" because their unavailability or failure can seriously jeopardize the operation of the national electric grid system, which can consequently be potentially harmful to the national industry. The share of large turbomachines in professional power sector markets varies depending on a specific country. As far as Poland is concerned, the most important part of the turbogenerators are units of +200 MW type (the 13K215 with 13 MPa live steam pressure, condensate operation unit and 215 MW of power output and its modifications up to the 13K242 – the same parameters, but almost a 15% increase in power output). This type of units is the most common large turboset to be found in Poland's power generation industry. As a matter of fact, over 50 such units have been in operation until the present time and they contribute to almost half of the national power production capabilities. The 18K360 appears to be another important type of turbosets, which is proven by the fact that there are 16 such units in Poland. Additionally, there are also several new units characterized by a very large power output ranging from 800 MW to +1, 000 MW. Taking the Polish power generation structure into account, the objective was formulated to focus firstly on +200 MW units.

Power generation machines are designed and expected to operate for long periods without the necessity of being shut down. Intervals between transient states, from start-up to coast-down, can be measured in months, or even longer timeframes in extreme cases. While being operated, a turbogenerator can be subjected to various operating conditions which can potentially cause fatigue or even damage of its components.

According to [1–3] and [4] the main and most common malfunctions include:

- unbalance,
- misalignment,
- rotor rub,
- oil-related and steam-related instabilities in bearings and seals respectively,
- bearing overload/ underload.

These malfunctions are hard to detect during steady-state operation of a turboset. Transient states of the machine, *i.e.* start-up and coast-down, provide significantly more valuable information in terms of a root cause diagnosis. The most important parameters to be assessed are natural frequencies of the shaft line. [5] presented an extensive study in this respect and emphasized the importance of analysing the lateral and torsional natural frequencies of a straight I-girder with trapezoidal web corrugations.

A typical 200 MW class turbogenerator consists of three cylinders (HP for *high pressure*, IP for *intermediate pressure*, and LP for *low pressure*) and one generator. The entire setup is presented in Fig. 1.

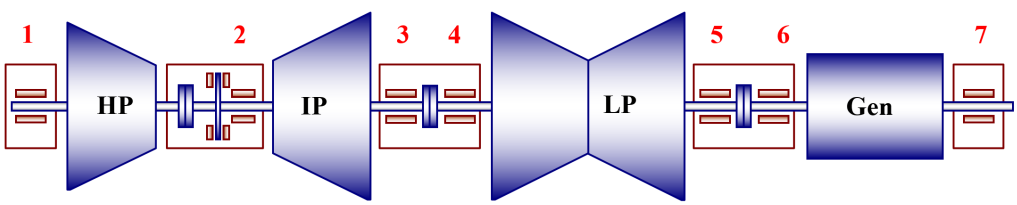

Fig. 1. The layout of a 200 MW type turboset. The bearings are numbered from the HP side (the figure prepared by the authors).

Metrol. Meas. Syst., Vol. 29 (2022), No. 1, pp. 175–190
DOI: 10.24425/mms.2022.138551

Generally speaking, professional power plants are large-sized facilities. A turbine hall itself can be as long as 0.5 km or even 1 km in extreme cases. A single turboset can be up to 40 m long, whereas a typical single plant has eight 200 MW units. Figure 2 illustrates an example of a turbine hall arrangement (top of the figure) and a turbine part cross-section (bottom of the figure).

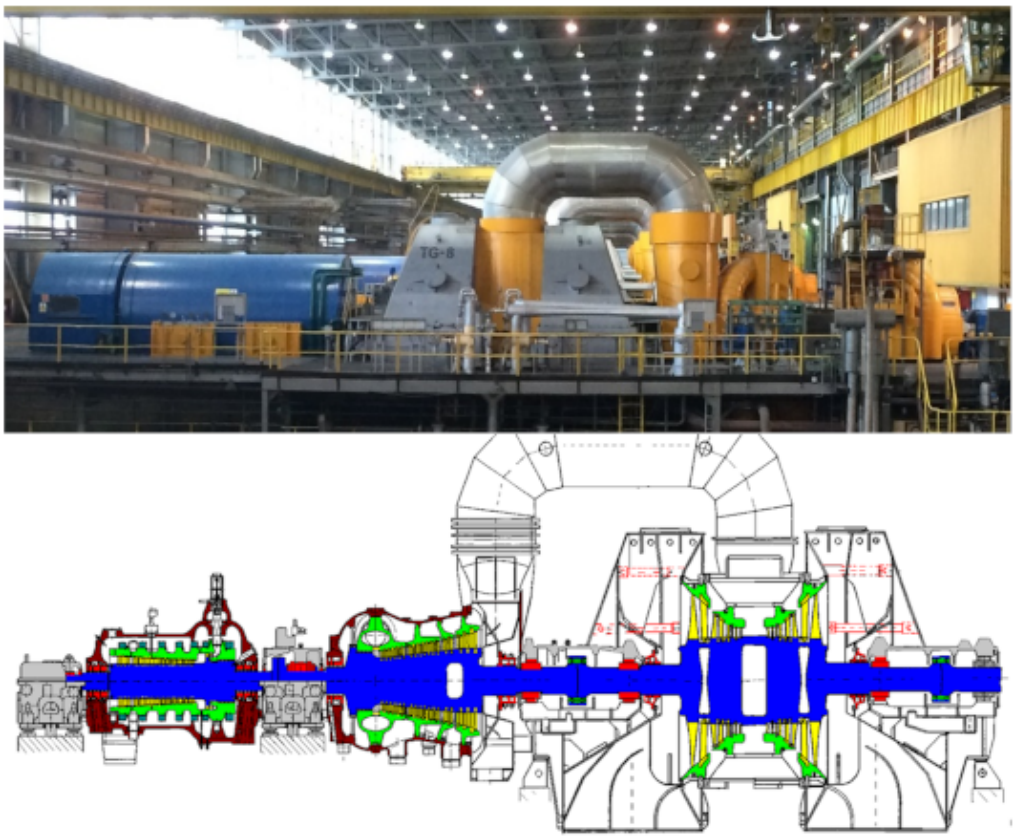

Fig. 2. A 13K215 type turbine unit installed in one of Polish power plants (top, the figure prepared by the authors) and the cross-section of such a turbine (bottom, the figure prepared by GE's R&D Department).

Vibration data are required to properly asses the technical condition of a rotor system. Critical machines are equipped with eddy current probes which can measure the vibration of the shaft within a journal bearing in two perpendicular axes (relatively to one another). Figure 3 depicts an arrangement of such probes. Performing an analysis involves taking into consideration several groups of parameters, *e.g.* broadband features, frequency selective features and harmonic vectors.

The field of rotordynamics has been intensively examined and researched starting from the early works of Jeffcott until the present-day literature. A very good introduction to the subject can be found in the widely recognized book by Bently and Hatch [2]. Interested readers can also refer to [6], where the full course of a rotordynamic analysis is given. In-depth and very detailed rotor modelling examples, in turn, can be found in [1] and [7]. Along with regular rotor models, they propose and explain several malfunctions, such as fluid inducted instabilities [1,2]. Complex and accurate models, especially focused on 200 MW class turbines, were proposed by Kiciński in [8] and [7]. To be more precise, his team developed advanced models which incorporated the

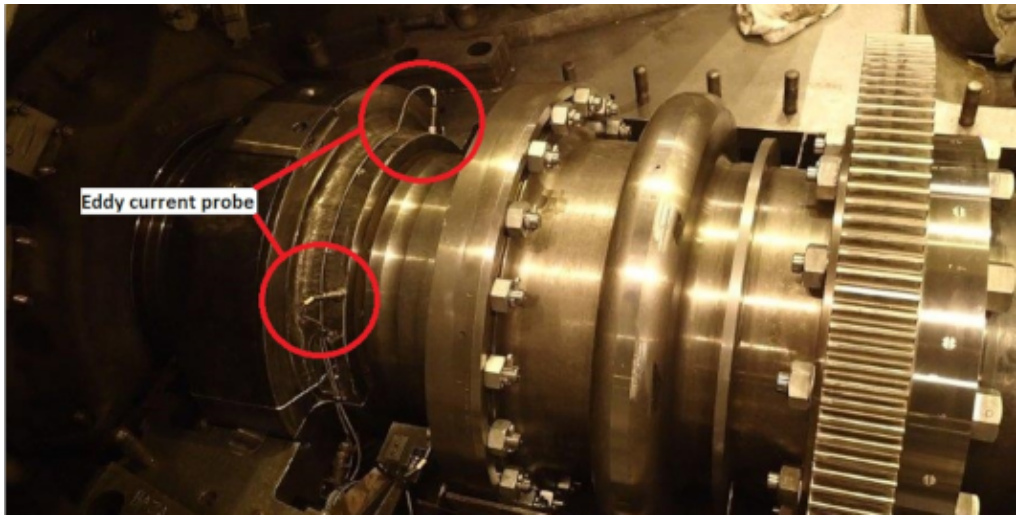

Fig. 3. An example of two types of proximity probe physical arrangement at the machine, inside a bearing pedestal. The probes are installed at +45° and +45° in the vertical direction (the figure prepared by the authors).

FEM (*Finite Element Method*) to analyse rotor behaviour. A rotor rub fault, on the other hand, requires a different approach to modelling, and the measurement of torsional vibration appears to be very helpful in this process. Interested readers can refer to [9], where such a study is presented in a very detailed manner.

The knowledge regarding the actual technical state, including the dynamic behaviour of a rotor, can bring many potential benefits. In this paper, the primary focus was put on the safety of operation. In a larger picture, however, the information about the actual dynamics of a rotor with blades can be used by designers to improve the machine performance. Interesting examples are revealed in [10] in relation to hydro turbine blades and in [11] in relation to gas turbine blades.

When it comes to vibration monitoring and protection, such units are typically equipped with 14 eddy current proximity probes (two probes at each of the bearings, as shown in Fig. 3). Often vibration velocity sensors are additionally installed at bearing casings. The exact setup varies between particular turbines (research objects), which is one of the reasons why the authors have decided to base the research on proximity probes.

The following assumptions must be made in terms of sampling and triggering data in order to collect transient data properly:

- sample after each $\Delta_{\text{rpm}} = \pm 10$ rpm (since the trigger is activated by each change of ±10 revolutions per minute in the rotational speed, the data will be stored in the acquisition unit. It does not matter when the trigger was activated along the rotational speed span regardless of the time elapsed between the samples),
- sample after each $\Delta_{\text{time}} = 20$ sec (after each 20 seconds, samples to be stored regardless of the rotational speed change).

Due to shaft line inertia during a transient state (especially during coast-downs), the data from 3,000 rpm to approximately 1,300 rpm will often be sampled by Δ_{rpm}, and from 1,300 rpm to the turning gear (which is activated at $\omega_{\text{rpm}} < 20$) rpm the main trigger will be Δ_{time}. As a result, the data is not evenly distributed in terms of both time and rpm value. Several issues must be overcome in order to use the actual data from the measurement:

Metrol. Meas. Syst., Vol. 29 (2022), No. 1, pp. 175–190
DOI: 10.24425/mms.2022.138551

– the "raw" samples are unevenly spread (the reason is the configuration of the sampling and is explained in the previous paragraph),
– due to operational reasons, the start point and end point of the measurement are not always the same,
– depending on the type of a transient (start-up or coast-down), the data is not shown in order (the rotational speed vector may start from the lowest rotational speed or, alternatively, from the highest one).

Even if the nature of the transient is the same, the starting point of triggering each transient is not always the same, particularly with respect to the rotational speed. The most important aspect is whether the starting point varies between particular measurements.

The paper is structured in the following manner. In Section 2, the DE (*Differential Evolution*) algorithm is described and used to obtain the best fit for decomposition of the function parameters into measured data. In Section 3, the fault identification method is proposed and its possibilities are discussed. Furthermore, an in-depth insight into transient decomposition representation as a sum of less complex signals is described and constitutes the most innovative characteristic of this paper. To be more precise, a set of initial parameters for the decomposed functions which are obtained from GE's commercial and professional rotor dynamic program is presented and the parameters are intended to act as a set of initial values for further investigations. Additionally, the MSE (*Mean Squared Error*) and the MAE (*Mean Absolute Error*) are defined and utilised to assess the fit of the received decomposed functions on the measured data. In Section 4, a step-by-step process for data gathering, data transformation and data decomposition into a set of several signals is demonstrated. Subsequently, some examples of transients in good condition are shown: one with moderate unbalance and one with excessive unbalance. Afterwards, a table of the aforementioned set of indicators and parameters is elaborated upon. Finally, Section 5 summarizes our findings and conclusions and some further steps to enhance our methods of identification are proposed.

2. Fault identification method

Large turbogenerators exhibit a highly non-linear response during transient states due to a variety of factors, such as: passage through its resonances, lube oil damping, fluid forces (*e.g.* steam), rubbing and others. In order to deal with such a complex response, the decision was taken to decompose each transient response into a set of signals by means of the structure known as "a priori", and such decomposed signals can be interpreted separately, thereby facilitating the analysis. To find the best solution, we decided to apply the DE algorithm, which provides promising results with multidimensional functions [12, 13].

Nonlinearity in a transient response, even in respect of a single rotor supported by two bearings, can cause some difficulties with reference to its description in a mathematical sense. One of the simplest ways can be found in [14], where a system is described as a mass supported by a spring and a damper on a vibrating base, which exhibits the behaviour observed during the transient shown in Fig. 4.

The next step of the analysis is to introduce a fundamental model of rotor lateral vibrations depicted in Fig. 5, thoroughly described and explained in [1], which can yield the transient state curves presented in Fig. 6.

If an external force comes only from an unbalance force, therefore $\varpi = \Omega$. Having that, the balance of generalized forces can be described as [1] and [7]:

$$M\ddot{x} + D_S\dot{x} + Kx = Fcos\,(\varpi t + \delta) + Pcos\gamma\,. \tag{1}$$

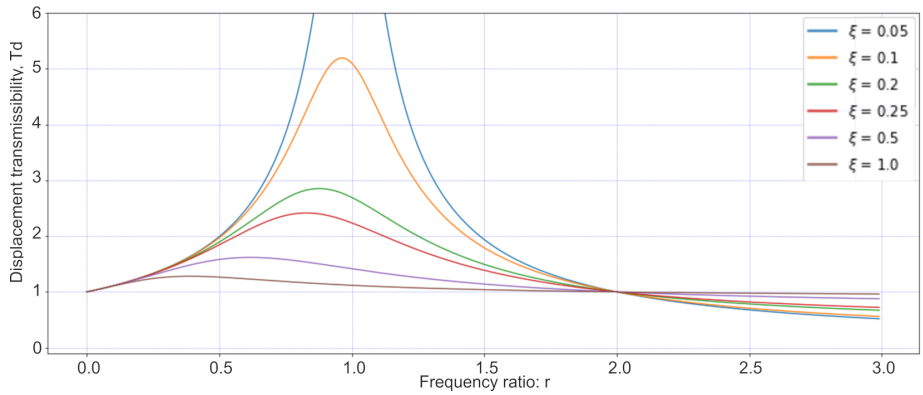

Fig. 4. Amplitude of a system during excitation frequency change according to the assumptions indicated in [14].

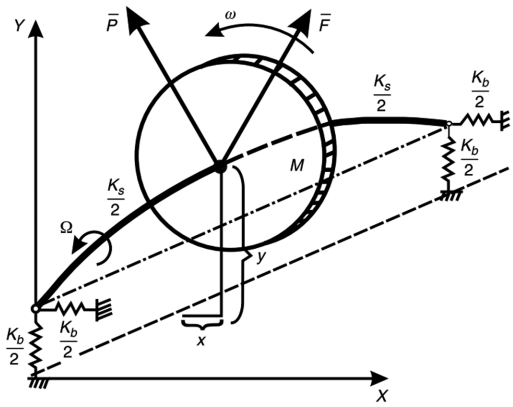

Fig. 5. First lateral mode of the isotropic rotor [1].

The amplitude and phase for a nonsynchronous vibration response are expressed by the following formulas:

$$B = \frac{F}{\sqrt{(K - M\omega^2)^2 + D_S^2\omega^2}}, \tag{2}$$

$$\beta = \delta + \arctan\frac{-D_S\omega}{K - M\omega^2} = \delta - \arctan\frac{D_S\omega}{K - M\omega^2}, \tag{3}$$

where: K_b, K_s – stiffness coefficients, M – mass/inertia coefficient, P – constant radial load force, F – rotating external exciting force, ω – frequency of externally applied force, Ω – rotational speed of the rotor, xy – coordinate system parameters, B – amplitude of the nonsynchronous vibration response, D_S – matrix of damping coefficients.

Figure 6 presents visualization of equations (2) and (3) during transient state amplitude and phase and these equations can be expressed with the following plots:

The transient state of a rotor is a highly nonlinear curve. In order to address a particular malfunction in the case of such a complex behaviour, its decomposition into a few known and less

Metrol. Meas. Syst., Vol. 29 (2022), No. 1, pp. 175–190
DOI: 10.24425/mms.2022.138551

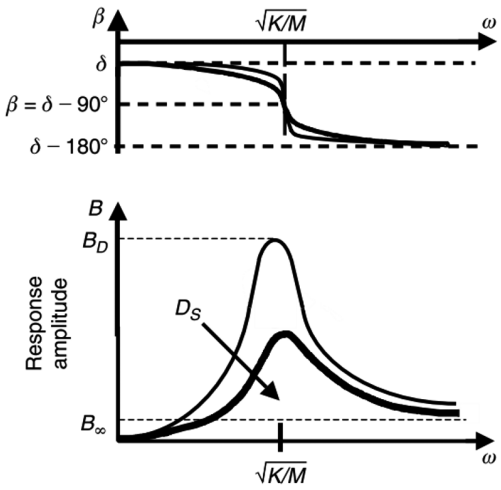

Fig. 6. Amplitude-phase plot of rotor response during change of the excitation force $F = mr\omega^2$ [1].

complex signals was proposed. The advantages of decomposition on nonlinear stochastic signals are well-known and thoroughly described in [13, 15] and [16]. Each of the decomposed signals represents a different rotor behaviour (malfunction) during the transient. Two types of functions have been offered by the authors for the purposes of approximating the transient signal:

$$f_1 = a_1 e^{\frac{(x-b_1)^2}{c_1}}, \tag{4}$$

$$f_2 = (a_2 x)^2 + b_2, \tag{5}$$

where:

f_1 – Gauss function with a_1, b_1, c_1 parameters respectively,
f_2 – parabola with a_2 parameter and b_2 as a bias term respectively,
a_1 – amplitude of the Gauss function,
b_1 – resonance peak inside the rotational speed interval,
c_1 – width of the resonance,
a_2 – factor related with synchronous response,
b_2 – bias constant (electrical/mechanical runout).

Basing on such an assumption, numerous function combinations with different sets of parameters can be superposed to fit the measured data.

Hence, the complex function described by equations (2) and (3) can be represented as a sum of the simple functions described by equations (4) and (5), similarly to the procedure described in [13] and [14]:

$$\varphi_{\text{approx}} = \varphi_1 + \varphi_2 + \ldots + \varphi_n = \sum_{i=1}^{n} \varphi_i, \tag{6}$$

where: φ_i – decomposed function described by equation (4) or (5) or by both equations.

Figure 7 presents an example of basic transient decomposition containing only two signals (Gaussian function and parabola), representing a single critical speed and unbalance component respectively.

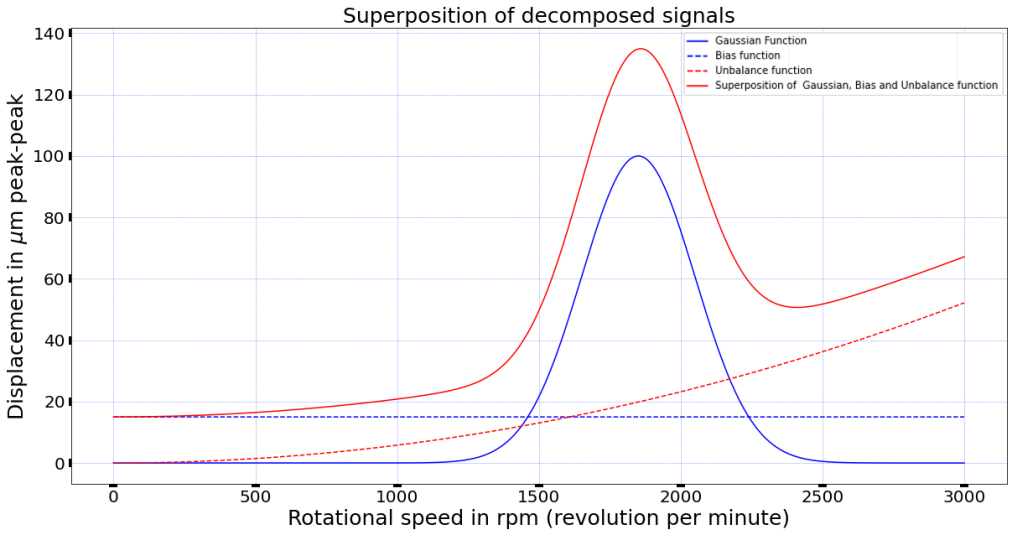

Fig. 7. Example of sum of decomposed signals simulating resonance and unbalance.

The MSE (*Mean Square Error*) and the MAE (*Mean Absolute Error*) are used as a measure of accuracy concerning the decomposition approximation. MSE_{tran} was defined as a sum of the squares, whereas MAE_{tran} was defined as a sum of the absolute values between real function φ_{real} and our approximation φ_{approx} within the space of all the samples throughout the transient in the equations (7) and (8) respectively. Consequently, the MSE_{tran} and the MAE_{tran} are used to assess a fit of the decomposed parts to the actual data which was obtained during the measurements:

$$MSE_{\text{tran}} = \sum_{\omega=1}^{N} \left[\varphi_{\text{real}}(\omega) - \sum_{i=1}^{n} \varphi_i(\omega) \right]^2, \tag{7}$$

$$MAE_{\text{tran}} = \sum_{\omega=1}^{N} \left| \varphi_{\text{real}}(\omega) - \sum_{i=1}^{n} \varphi_i(\omega) \right|, \tag{8}$$

where: ω – revolution per minute (rotational speed).

One Gaussian function with a parabola does not fit very well the transients from a real large machine, such as a turboset with the output power of +200 MW. A more realistic model needs to be applied in order to get reliable results. Thus, a combination of three Gaussian functions, a parabola plus a bias term was used, as described by equations (4) and (5).

The proposed method yields 11 parameters which can describe a single transient with three resonance peaks, unbalance and run-out. Each resonance is described by three parameters which can be monitored independently for the resonance peak, its placement along the rotational speed interval and the width related to damping in a bearing. To monitor the unbalance response, two parameters of a single parabola are needed. According to the tests carried out on a reference set of data, a set of the 11 parameters described above should suffice to properly model and monitor the transients and their most essential parameters.

Metrol. Meas. Syst., Vol. 29 (2022), No. 1, pp. 175–190
DOI: 10.24425/mms.2022.138551

3. Genetic and Differential Evolution Algorithm

Machine learning methods have been used for a relatively long period of time to model and detect faults of rotating machinery. There are numerous papers whose authors propose the application of machine learning methods – most frequently *Artificial Neural Networks* (ANN). Interested readers can find specific examples in the work of Rex *et al.*, who propose enhanced ANNs for a fault diagnosis of spur gears [17] Another example is [16] where ANNs are used to detect faults of complex epicyclic gearboxes. Applications of ML for large turbomachinery are less frequent and therefore, in the authors' opinion, this paper can be a valuable contribution.

Genetic Algorithms (GA) are parallel mathematical algorithms which transform each population (*i.e.* individual parameters of mathematical objects) into a new set of parameters on the basis of a fitness function. The fitness function is a way of evaluating the cost of an individual and population in order to adapt to the environment related to each population and its parameters. They are based on Darwin's theory of evolution which stated that only the best adapted individuals (the fittest ones) will survive to reproduce and create a new population which would be better adapted to the natural conditions. [18] describes the basics of GAs and delivers an extensive discussion on their advantages and limitations. The main advantage of the GA is its possibility to adapt to different problem solving tasks. [19] presents a GA enhancement and reinforcement in order to feature an extraction and classification algorithm based on the neural network used to diagnose electrocardiogram signals. [20] and [21] presents an interesting application of the Differential Evolution Algorithm to optimize rotating machinery, namely hydro turbines. In the paper, five different primary hydrofoil families were optimized and scaled. The optimized hydrofoils were found to deliver successful performance for hydrokinetic turbines.

The *Differential Evolution* (DE) is an evolutionary algorithm which constitutes part of the GA family. As a matter of fact, the DE is a stochastic search algorithm based on the population. What is more, the DE is based on Darwin's theory of evolution, where the strongest (*i.e.* fittest) and therefore the best individual has the best chance to survive and reproduce. The "fittest" parents from the population pass on their genes (qualities) to the next population which has a greater chance of survival, accommodation and reproduction, even higher than their parents have in a given environment. An example of such an approach was described in [12]. Further implementations and enhancements of the DE algorithm are presented in [22] and [23].

The aforementioned algorithm is used in the so-called "derivative-free optimization". In fact, the DE algorithm finds a minimum of a function $f(x)\colon R^n \rightarrow R$ where it is hard to approximate the derivatives of an analytical function (which may be complex or non-derivative), or it is impossible to identify the analytical form of a target function to be optimized and therefore the derivatives cannot be computed easily.

The DE algorithm has the following steps (its visual description is shown in Fig. 8):

1. Create a population with a *Np* individuals. Each individual has a set of parameters x. Each parameter vector corresponds to an objective function. Select a target and base vector.
2. Randomly select two population members.
3. Compute a weighted difference vector from the previously picked two parameter vectors.
4. Add a computed weighted difference vector to the base vector, thereby creating a mutant vector. Use the target vector and mutant vector for a crossover (trial vector).
5. Select from the two vectors, *i.e.* the target vector or trial vector (selection is based on the cost function).
6. Consequently, a new population is created.

The DE algorithms were used for the purposes of our research (depicted in Fig. 8).

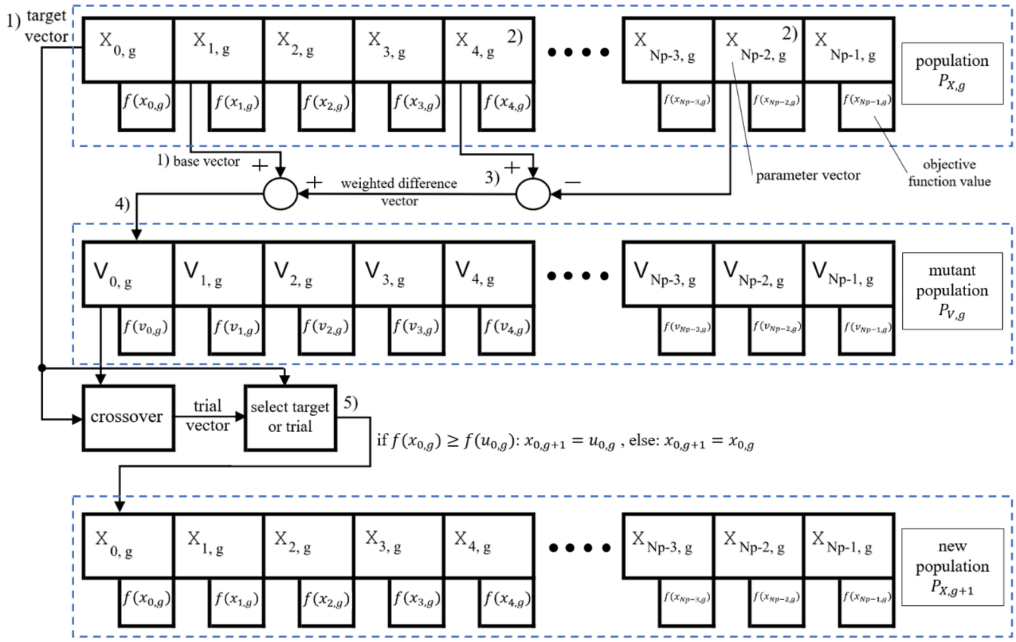

Fig. 8. Scheme of the Differential Evolution (DE) algorithm.
where: g – generation counter (increases with every algorithm cycle), $x_{Np-i,g}$ – parameter vector for the $Np - i$, $i \in 0, 1, 2 \ldots Np$ population member, $f\,(x_{Np-i,g})$ – objective function value for the parameter vector $x_{Np-i,g}$, $v_{Np-i,g}$ – parameter vector for the $Np - i$, $i \in 0, 1, 2 \ldots Np$ mutant population member, $f\,(v_{Np-i,g})$ – objective function value for the mutant parameter vector $v_{Np-i,g}$

4. Case study

The subject of the case study was a 13K215 turbine unit coupled with a generator characterised by the power output of 230 MW, whereby the turbine unit is located in one of the Polish power plants. Figure 9 presents an example setup of a vibration measurement course and a list of sensors used for the analysis during the measurements. Due to the huge amount of the data obtained at each measurement, showing the most explicit example appears to be reasonable in this context. Consequently, Fig. 10 summarizes and presents the 1st harmonic response of the machine during nine transient states with different technical states (damping of the bearings).

To simplify the problem, only the data from a single transducer was used at the initial stage of the research, as shown in Fig. 10. Basing on the set of nine transient data states, the DE algorithm was implemented in order to find the best fit for the decomposed curve. As explained in the previous section, three Gaussian functions, one parabola and the bias term were used to model the decomposition functions. In this configuration, two separate critical zones/intervals and their combination can be modelled. The third Gaussian component is an addition to properly model a wide range of response changes. The parabola coefficients are used to determine unbalance severity during the transient. The bias term, on the other hand, is used to model the initial conditions of the measurements (*e.g.* as an initial mechanical and electrical run-out).

This case study consists of two different transients conditions:

– transient named U2_09 in Fig. 10 – the best case scenario,
– transient named U2_01 in Fig. 10 – the worst case scenario.

Metrol. Meas. Syst., Vol. 29 (2022), No. 1, pp. 175–190
DOI: 10.24425/mms.2022.138551

CH#	Channel Name	Machine Name	Status	Angle	Speed Units(P)	Amp Unit	Phas
1	1X		OK	45°	rpm	um pp	deg
2	1Y		OK	45°	rpm	um pp	deg
3	2X		OK	45°	rpm	um pp	deg
4	2Y		OK	45°	rpm	um pp	deg
5	3X		OK	45°	rpm	um pp	deg
6	3Y		OK	45°	rpm	um pp	deg
7	4X		OK	45°	rpm	um pp	deg
8	4Y		OK	45°	rpm	um pp	deg
9	5X		OK	45°	rpm	um pp	deg
10	5Y		OK	45°	rpm	um pp	deg
11	6X		OK	45°	rpm	um pp	deg
12	6Y		OK	45°	rpm	um pp	deg
13	7X		OK	45°	rpm	um pp	deg
14	7Y		OK	45°	rpm	um pp	deg
15	1H		OK	90°	rpm	mm/s rms	deg
16	2H		OK	90°	rpm	mm/s rms	deg
17	3H		OK	90°	rpm	mm/s rms	deg
18	4H		OK	90°	rpm	mm/s rms	deg
19	4V		OK	0°	rpm	mm/s rms	deg
20	5H		OK	90°	rpm	mm/s rms	deg
21	5V		OK	0°	rpm	mm/s rms	deg
22	6H		OK	90°	rpm	mm/s rms	deg
23	7H		OK	90°	rpm	mm/s rms	deg
24	Power Channel		OK	0°	rpm	W	deg
25	Keyphasor Channel 1	Generator	OK	90°	rpm	V pp	deg

Fig. 9. Vibration measurement setup: left – acquisition units; right – the list of sensors included in the analysis during re-commissioning.

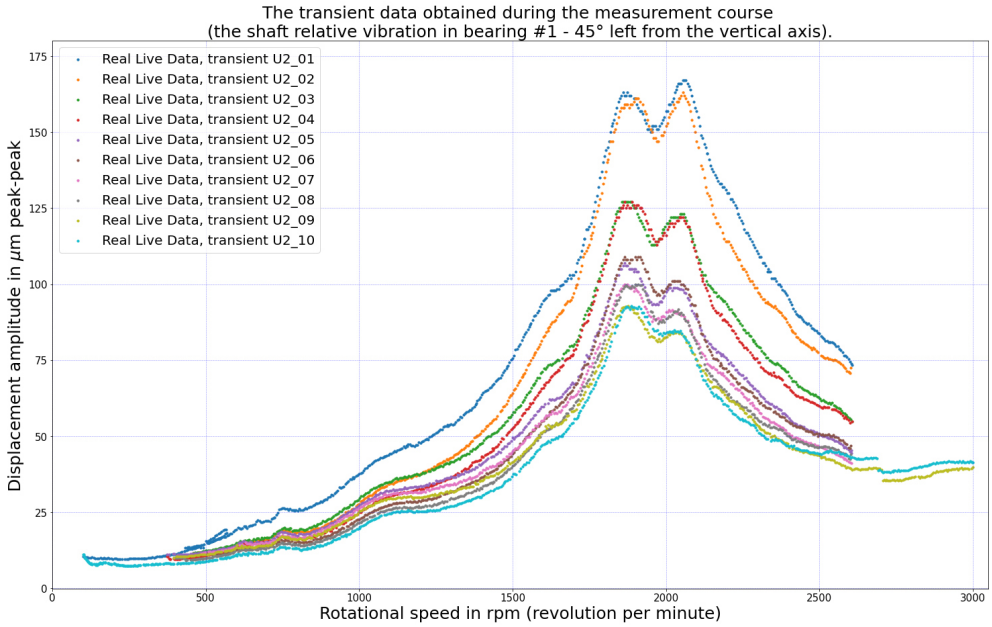

Fig. 10. Transient data obtained during the measurement course (the shaft relative vibration in bearing #1 – 45° left from the vertical axis.

The analysed parameter was the vibration amplitude recorded during the transient state.

The DE algorithm was used to establish the parameters for the decomposed functions. The parameters for the DE as an optimizing algorithm are as follows:

– "rand": The vectors/individuals are randomly chosen. Each vector/individual from the pool (entire population) has the same chance of being chosen.
– "1": As a mutation scheme – one vector difference is taken into account for mutation of the vector.
– "bin": The crossover strategy to mix the target and trial vectors: the binominal crossover.

Table 1 summarizes the influence and trade-off between the population size and the number of evolutions. The two fitness parameters, *i.e.* the MSE and the MAE, were used to assess the performance of the DE algorithm.

Table 1. Parameter list of decomposed function for the measurement data U2_09.

Parameter list of decomposed function	**Population: 20 Evolutions: 500**	**Population: 40 Evolutions: 500**	**Population: 40 Evolutions: 1000**	**Population: 40 Evolutions: 3000**
Gauss 1 amplitude	$1.00e+00$	$4.42e+01$	$4.59e+01$	$4.10e+01$
Gauss 1 resonance	$1.23e+03$	$1.94e+03$	$2.14e+03$	$1.95e+03$
Gauss 1 width	$1.95e+02$	$2.02e+02$	$9.79e+02$	$2.04e+02$
Gauss 2 amplitude	$-1.74e+01$	$-9.04e-01$	$0.00e+00$	$-1.35e+01$
Gauss 2 resonance	$1.00e+03$	$1.00e+03$	$2.50e+03$	$2.50e+03$
Gauss 2 width	$5.00e+02$	$2.00e+01$	$4.08e+02$	$5.00e+02$
Gauss 3 amplitude	$4.86e+01$	$4.40e+01$	$4.21e+01$	$5.30e+01$
Gauss 3 resonance	$1.92e+03$	$2.17e+03$	$1.93e+03$	$2.30e+03$
Gauss 3 width	$2.60e+02$	$1.04e+03$	$1.99e+02$	$9.22e+02$
Parabola factor	$1.00e-08$	$1.00e-08$	$1.00e-08$	$1.00e-08$
Bias term	$3.80e+01$	$0.00e+00$	$0.0000e+00$	$3.46e+00$
MSE	4.2165	2.2421	2.39213	2.39214
MAE	4.3619	1.8759	1.6794	1.5741

A smaller population (*e.g.* 20 vectors/individuals) cannot produce decomposition parameters which can replicate the transient function well enough. In this arrangement, the MSE and MAE cost functions score above 4.2 and 4.3, respectively. Increasing the population by a factor of two helped reduce the costs, but several attempts performed with 500 evolutions proved that such a small evolution rate does not always suffice to properly replicate the transient state complexity in detail.

The best performance in terms of repeatability of the outcome with regard to the MSE and the MAE and the values of the decomposed parameters resulted in the following setup of the DE algorithm inputs:

- Population size: 40;
- No. evolutions: 1000;
- Crossover parameter: 0.7;
- Mutation parameter: 1.2.

It can be stated that the best configuration of the population and evolution parameters in this particular case is 40 and between 1,000 and 2,000, respectively.

Figure 11 depicts a set of examples of from our case study. The authors used MAE as a performance evaluation function for the top and bottom left plot, and MSE as the right side plots. MAE cost function performs well for smaller amplitudes values and its performance is similar to MSE which can be seen in Fig. 10 (the upper left and right curves). The red line in both these plots is almost identical. On the other hand, the MSE is superior to the MAE when it comes to higher amplitude values and more complex curve shape decomposition. The red line in (the lower right), where the MSE was used as the fitness function, replicates a given transient much better than the one on the left-hand side of the Table 2 (where the MAE was used).

Metrol. Meas. Syst., Vol. 29 (2022), No. 1, pp. 175–190
DOI: 10.24425/mms.2022.138551

Table 2 summarizes the parameters of the two bottom plots illustrated in Fig. 11. The results suggest that the cost function based on the MSE is superior to that based on the MAE. The parameters obtained by means of the MSE describe the transient with two peaks near to each other in contrast to the MAE which was not able to achieve the shape of the actual data.

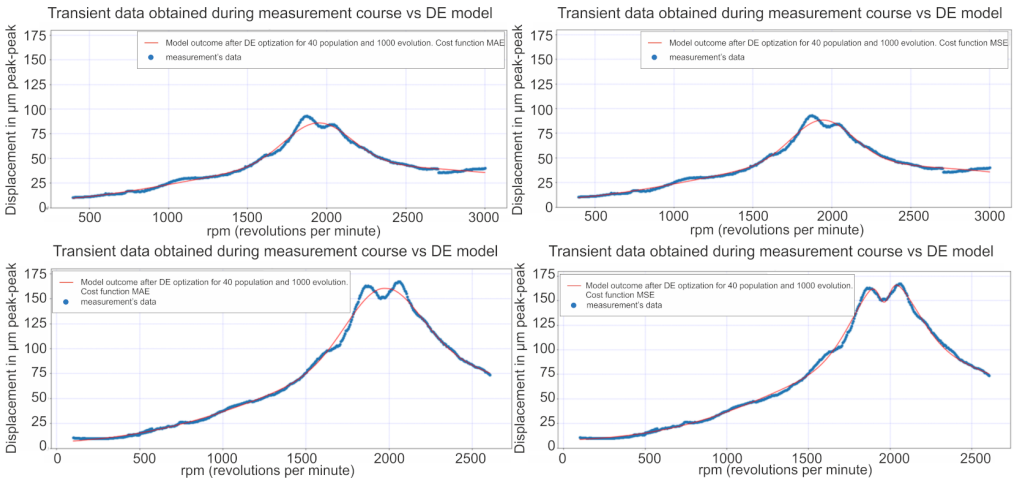

Fig. 11. Curve fitting examples of the decomposed signals and the transient measured. The plots present: top left – the low amplitude and the MAE cost function; top right – the low amplitude and the MSE cost function; bottom left – the high amplitude and the MAE cost function; bottom right – the high amplitude and the MSE cost function.

Table 2. Parameters list of decomposed function for the U2_01 transient's data.

Parameter list of decomposed function	**Population: 40 Evolutions: 1000 Cost function: MAE**	**Population: 40 Evolutions: 1000 Cost function: MSE**
Gauss 1 amplitude	$2.08e+02$	$7.90e+01$
Gauss 1 resonance	$2.27e+03$	$1.97e+03$
Gauss 1 width	$4.98e+02$	$1.86e+02$
Gauss 2 amplitude	$-1.16e+02$	$-2.39e+01$
Gauss 2 resonance	$2.43e+03$	$1.97e+03$
Gauss 2 width	$2.71e+02$	$3.38e+01$
Gauss 3 amplitude	$2.20e+01$	$8.83e+01$
Gauss 3 resonance	$1.00e+03$	$2.08e+03$
Gauss 3 width	$3.25e+02$	$7.43e+02$
Parabola factor	$1.00e--08$	$1.00e--08$
Bias term	$7.64e+00$	$6.00e+00$

5. Summary and conclusions

In the paper, the method for automatic decomposition of the transient vibration data into the components that consist of Gaussians and polynomial/quadratic parts with the bias term was proposed. As a result, the method yields 11 parameters for the four components of the original

transient. Thus, such an output vector is much smaller than the original data set and appears to be much better for the purposes of the analysis. It is worth emphasizing that the result parameters have a physical meaning and can be understood better.

The decomposed transient parts are responsible for particular failure modes and, as a consequence, not only can different malfunctions be detected, but they can also be identified, which, in the authors' opinion, is the main novelty of the paper.

The DE algorithm was successfully applied to the automatically obtained parameters of the decomposed functions. Looking at the issue from another perspective, the paper proposes a method for modelling transient data by means of a subset of functions. The DE algorithm is used as a method for obtaining the model parameters.

The method has been validated on the actual data originating from a 200 MW class turbine. The case study presents an example of bearing damping changes which result in a large difference in relation to the dynamic response of the machine. The main finding of the case study was the indication of the manner in which various error functions influence the modelled parameters. It has been observed that the MSE is suited better than the MAE due to the fact that the MSE is capable of modelling the non-trivial case of two resonances located close to one another. It must be also highlighted that the difference is not visible when the vibration amplitude is smaller as the dataset is thereby simpler.

In further research, the GA algorithm will be used in order to potentially enhance the outcome accuracy of the method. We will examine various configurations of the DE algorithm, particularly the mutation strategy.

Moreover, the intention is also to use the data from various malfunctions, the first of which will be related to unbalance. The internal GE Engineering Program will be applied in order to establish a set of parameters of the decomposed functions and the resulting vibration data is to be compared with the program parameters. In the subsequent steps, various types of malfunction will be added, *e.g.* bearing malfunctions such as the oil whirl.

Acknowledgements

This paper is partially supported by grant No. POIR.04.01.04-00-0080/19, funded by the National Centre for Research and Development (Poland). Moreover, the authors would also like to express their gratitude to GE for sharing the engineering data and providing an opportunity to collect transient data from a real turboset.

References

[1] Muszynska, A. (2005). *Rotordynamics*. CRC Press. https://doi.org/10.1201/9781420027792

[2] Bently, D. E., Hatch, C. T., & Grissom, B. (2002). *Fundamentals of Rotating Machinery Diagnostics*. ASME Press. https://asmedigitalcollection.asme.org/ebooks/book/1/Fundamentals-of-Rotating-Machinery-Diagnostics

[3] Adams, M. L. (2009). *Rotating Machinery Vibration: From Analysis to Troubleshooting,* (2nd ed.). CRC Press. https://doi.org/10.1201/9781439847558

[4] Eisenmann, R. C. (1997). *Machinery Malfunction Diagnosis and Correction: Vibration Analysis and Troubleshooting for Process Industries* (1st ed.). Prentice Hall. https://www.abebooks.co.uk/Machinery-Malfunction-Diagnosis-Correction-Vibration-Analysis/30897131746/bd

Metrol. Meas. Syst., Vol. 29 (2022), No. 1, pp. 175–190
DOI: 10.24425/mms.2022.138551

[5] Vo, D.-Q., & Ton-That, H. L. (2020). Free vibration of simply supported steel I-girders with trapezoidal web corrugations. *Reports in Mechanical Engineering*, *1*(1), 141–150. https://doi.org/10.31181/rme200101141v

[6] Vance, J. M., Zeidan, F. Y., & Murphy, B. T. (2010). *Machinery Vibration and Rotordynamics* (2nd ed.). Wiley & Sons. https://www.wiley.com/en-cr/Machinery+Vibration+and+Rotordynamics-p-9780471462132

[7] Kiciński, J. (2006). *Rotor Dynamics* (2nd ed.). Institute of Fluid-Flow Machinery Polish Academy of Science.

[8] Kiciński, J. (2005). *Dynamika Wirników i Łożysk Ślizgowych. Polish (Dynamics of shafts and hydrodynamic bearings)* (E. B. Burka, Ed.; Szewalski Institute of Fluid-Flow Machinery). Institute of Fluid-Flow Machinery Polish Academy of Science.

[9] Hajnayeb, A., Shirazi, K. H., & Aghaamiri, R. (2020). Vibration measurement for crack and rub detection in rotors. *Metrology and Measurement Systems*, 65–80. https://doi.org/10.24425/mms.2020.131719

[10] Mastrogiannakis, I., & Vosniakos, G.-C. (2020). Exploring structural design of the Francis hydroturbine blades using composite materials. *Facta Universitatis, Series: Mechanical Engineering*, *18*(1), 043–055. https://doi.org/10.22190/FUME190609001M

[11] Akzhigitov, D., Srymbetov, T., Aldabergen, A., & Spitas, C. (2021). Structural and Aerodynamical Parametric Study of Truss-Core Gas Turbine Rotor Blade. *Journal of Applied and Computational Mechanics*, *7*(2), 831–838. https://doi.org/10.22055/jacm.2020.35467.2667

[12] Storn, R., & Price, K. (1997). Differential Evolution – A Simple and Efficient Heuristic for Global Optimization over Continuous Spaces. *Journal of Global Optimization*, *11*(4), 341–359. https://doi.org/10.1023/A:1008202821328

[13] Chui, C. K., & Mhaskar, H. N. (2016). Signal decomposition and analysis via extraction of frequencies. *Applied and Computational Harmonic Analysis*, *40*(1), 97–136. https://doi.org/10.1016/j.acha.2015.01.003

[14] Rao, S. S. (2017). *Mechanical Vibrations* (6th ed.). Pearson. https://www.pearson.com/content/one-dot-com/one-dot-com/us/en/higher-education/program.html

[15] Cicone, A. (2019). Nonstationary Signal Decomposition for Dummies. *Advances in Mathematical Methods and High Performance Computing*, *41*, 69–82. https://doi.org/10.1007/978-3-030-02487-1_3

[16] Dworakowski, Z., Dziedziech, K., & Jabłoński, A. (2018). A novelty detection approach to monitoring of epicyclic gearbox health. *Metrology and Measurement Systems*, *25*(3), 459–473. https://doi.org/10.24425/123896

[17] Krishnakumari, A., Rex, F. M. T., Andrews, A., & Hariharasakthisudhan, P. (2020). A hybrid approach for fault diagnosis of spur gears using Hu invariant moments and artificial neural networks. *Metrology and Measurement Systems*, *27*(3), 451–464. https://doi.org/10.24425/mms.2020.134587

[18] Koza, J. R., & Poli, R. (2005). Genetic Programming. In E. K. Burke & G. Kendall (Eds.). *Search Methodologies: Introductory Tutorials in Optimization and Decision Support Techniques* (pp. 127–164). Springer US. https://doi.org/10.1007/0-387-28356-0_5

[19] Li, H., Yuan, D., Ma, X., Cui, D., & Cao, L. (2017). Genetic algorithm for the optimization of features and neural networks in ECG signals classification. *Scientific Reports*, *7*(1), 41011. https://doi.org/10.1038/srep41011

[20] Muratoglu, A., & Yuce, M. I. (2017). Design of a River Hydrokinetic Turbine Using Optimization and CFD Simulations. *Journal of Energy Engineering*, *143*(4), 04017009. https://doi.org/10.1061/(ASCE)EY.1943-7897.0000438

[21] Muratoglu, A., Tekin, R., & Ertuğrul, Ö. F. (2021). Hydrodynamic optimization of high-performance blade sections for stall regulated hydrokinetic turbines using Differential Evolution Algorithm. *Ocean Engineering*, *220*, 108389. https://doi.org/10.1016/j.oceaneng.2020.108389

[22] Qin, A. K., Huang, V. L., & Suganthan, P. N. (2009). Differential Evolution Algorithm with Strategy Adaptation for Global Numerical Optimization. *IEEE Transactions on Evolutionary Computation*, *13*(2), 398–417. https://doi.org/10.1109/TEVC.2008.927706

[23] Das, S., Mullick, S. S., & Suganthan, P. N. (2016). Recent advances in differential evolution – An updated survey. *Swarm and Evolutionary Computation*, *27*, 1–30. https://doi.org/10.1016/j.swevo.2016.01.004

Tomasz Barszcz received his M.Sc. in electronic engineering and his Ph.D. in mechatronics from the Gdańsk University of Technology in 1993 and 1997 respectively. He is currently Professor at the AGH University of Science and Technology. He has had long experience of working with power generation companies, e.g. ABB, ALSTOM and GE. His main research interests are new machinery diagnostics methods and new technologies of condition monitoring systems. He is the author of over 250 papers and books on machinery diagnostics. Monitoring systems developed under his supervision were installed on several hundred machines worldwide. He is a co-founder and CXO of several companies in the field of condition monitoring.

Mateusz Zabaryłło received his M.Sc. in electronic engineering from the Gdańsk University of Technology in 2008. He has had extensive practice in applied diagnostic (since 2009). He is currently enrolled in an industry-based Doctorate program in cooperation with the GE company where he works. He supervised shaftline and bearings assembly in both newly commissioned and repaired/modernized machines across Poland and abroad. He assists in commissioning of large turbomachinery by vibration's measurements, analysis, expertise and on-site balancing.